



## Mapping the interaction site for $\beta$ -arrestin-2 in the prokineticin 2 receptor

R. Lattanzi<sup>a</sup>, I. Casella<sup>b</sup>, M.R. Fullone<sup>c</sup>, M. Vincenzi<sup>a</sup>, D. Maftai<sup>a</sup>, R. Miele<sup>c,\*</sup>

<sup>a</sup> Department of Physiology and Pharmacology "Vittorio Erspamer", Sapienza University of Rome, Piazzale Aldo Moro 5, I-00185 Rome, Italy

<sup>b</sup> Dipartimento del Farmaco, Istituto Superiore di Sanita, I-00161 Rome, Italy

<sup>c</sup> Department of Biochemical Sciences "A. Rossi Fanelli", Sapienza University of Rome, Piazzale Aldo Moro 5, I-00185 Rome, Italy

### ARTICLE INFO

#### Keywords:

G-protein coupled receptors  
 $\beta$ -Arrestin-2  
Prokineticin receptors

### ABSTRACT

G protein-coupled receptors (GPCRs) are a family of cell membrane receptors that couple and activate heterotrimeric G proteins and their associated intracellular signalling processes after ligand binding. Although the carboxyl terminal of the receptors is essential for this action, it can also serve as a docking site for regulatory proteins such as the  $\beta$ -arrestins. Prokineticin receptors (PKR1 and PKR2) are a new class of GPCRs that are able to activate different classes of G proteins and form complexes with  $\beta$ -arrestins after activation by the endogenous agonists PK2. The aim of this work was to define the molecular determinants within PKR2 that are required for  $\beta$ -arrestin-2 binding and to investigate the role of  $\beta$ -arrestin-2 in the signalling pathways induced by PKR2 activation. Our data show that PKR2 binds constitutively to  $\beta$ -arrestin-2 and that this process occurs through the core region of the receptor without being affected by the carboxy-terminal region. Indeed, a PKR2 mutant lacking the carboxy-terminal amino acids retains the ability to bind constitutively to  $\beta$ -arrestin-2, whereas a mutant lacking the third intracellular loop does not. Overall, our data suggest that the C-terminus of PKR2 is critical for the stability of the  $\beta$ -arrestin-2-receptor complex in the presence of PK2 ligand. This leads to the  $\beta$ -arrestin-2 conformational change required to initiate intracellular signalling that ultimately leads to ERK phosphorylation and activation.

### 1. Introduction

G protein-coupled receptors (GPCRs) are the largest family of receptors on cell membranes and represent an important class of drug targets. In response to the binding of ligand, GPCRs activate G proteins as a guanine nucleotide exchange factor that triggers downstream signalling processes. Termination of G protein-mediated signalling is achieved by specific kinases that phosphorylate residues in the carboxy-terminal (C-terminal) tail and intracellular loops of the receptor. This action leads to the recruitment of  $\beta$ -arrestins, which subsequently initiate second wave of  $\beta$ -arrestins-mediated signalling [1].

Arrestins are a small family of four homologous proteins including of two visual arrestins (arrestin-1 and arrestin -4) and two ubiquitous proteins, (arrestin-2 and arrestin-3) also known as  $\beta$ -arrestin-1 and  $\beta$ -arrestin-2. Remarkably, all vertebrate arrestins have very similar structures in their basal conformation, characterized by two domains, commonly referred to as N- and C-domains. It has been shown that the binding of  $\beta$ -arrestin to receptors occurs at two different sites. Firstly, there is an interaction between a positively charged N-terminal domain of  $\beta$ -arrestin and the phosphorylated C-tail of the receptor. This leads to

$\beta$ -arrestin reaching its active state by twisting its domains and releasing the arrestin tail. The second interaction instead takes place between the  $\beta$ -arrestin finger loop and the activated receptor core. Binding of  $\beta$ -arrestin to the receptor leads to desensitization and, in some cases, internalization of GPCRs. It is already known that  $\beta$ -arrestin acts as a scaffold for interactions with numerous protein partners and mediates signalling transduction via mitogen-activated protein kinase (MAPK)-mediated phosphorylation of extracellular signal-regulated kinase 1/2 (ERK<sub>1/2</sub>) [2,3]. Prokineticin 2 (PK2) binds two related GPCRs called prokineticin receptors (PKRs). Both PKRs couples to different class of G-proteins, G<sub>αq/11</sub>, G<sub>αs</sub> and G<sub>αi</sub> and mediates several signalling pathways that promote an increase in intracellular calcium and cAMP levels, phosphorylation of Akt and activation of ERK and STAT3 [4,5]. The diversity of G proteins coupled to PKRs as well as the alternative splicing isoforms of PK2 [6–8] and prokineticin receptor 2 (PKR2) [9], dimerization of PKR2 and interaction with accessory proteins [10–12] contribute significantly to the modulation of receptor-specific functional properties, including ligand binding, signal transduction and trafficking. The prokineticin system is expressed in a variety of organs, including the central and peripheral nervous system, heart, ovaries, testes, placenta,

\* Corresponding author.

E-mail address: [rossella.miele@uniroma1.it](mailto:rossella.miele@uniroma1.it) (R. Miele).

<https://doi.org/10.1016/j.cellsig.2024.111175>

Received 26 January 2024; Received in revised form 4 April 2024; Accepted 10 April 2024

Available online 15 April 2024

0898-6568/Published by Elsevier Inc. This is an open access article under the CC BY license (<http://creativecommons.org/licenses/by/4.0/>).

adrenal cortex, peripheral blood cells and bone marrow [13]. Such widespread distribution suggests that the PK2/PKR system exert various tissue-specific biological functions, such as angiogenesis, neurogenesis, haematopoiesis, hormone secretion, regulation of circadian rhythm and modulation of food intake and drinking, as well as in pathological conditions such as pain, cancer, obesity, neurodegenerative diseases such as Alzheimer's and Parkinson's disease and Kallmann syndrome [14–18]. Using BRET techniques, it has been shown that both PKR1 and PKR2 form complexes with  $\beta$ -arrestins [19,20] and that binding of  $\beta$ -arrestins determines receptor desensitization but not endocytosis. In fact, agonist-induced PKR2 endocytosis has been proved to be  $\beta$ -arrestins independent although mediated by GRK2 and the clathrin pathway [21].

The aim of this work was to define the molecular determinants within PKRs that are required for  $\beta$ -arrestin-2 binding and to analyse  $\beta$ -arrestin-2-induced ERK activation. The results show that  $\beta$ -arrestin-2 is able to constitutively bind the PKR2 and that this basal binding is mediated by the core region, whereas it is not affected by the presence of the C-terminal region. In contrast, the data show that the receptor C-terminal region is required for  $\beta$ -arrestin-2 to bind activated PKR2 and in turn for  $\beta$ -arrestin2-mediated ERK activation. This study may allow the identification of new specific targets for potential new drugs useful for the treatment of the various diseases correlated with the prokineticin system.

## 2. Materials and methods

### 2.1. Drugs and reagents

Dulbecco's Modified Eagle Medium with F-12 supplement (DMEM/F-12), foetal bovine serum, phosphatases inhibitor cocktails, penicillin were purchased from Sigma Aldrich. All enzymes used for molecular cloning and an enhanced chemiluminescence detection kit were from Roche Molecular Biochemicals. All other chemicals used for SDS-polyacrylamide gel electrophoresis and Western blotting were purchased from Bio-Rad. Primary antibody used: mouse polyclonal antibody anti-PKR2 (sc-365,696), against the amino-terminal region of PKR2 from Santa Cruz Biotechnology; mouse monoclonal antibody anti-FLAG (F1804) and anti-polyHistidine–Peroxidase (A7058) from Sigma Aldrich, rabbit polyclonal antibody anti-ERK (#44–654) and anti-pERK (#44–680) from Invitrogen. Nitrocellulose membranes (0.45  $\mu$ m; Hybond-C Extra) were from Amersham Pharmacia Biotech, Coelenterazine 400a was from NonoLight.

### 2.2. Expression plasmids

The construct pcDNA PKR2 was previously described [7]. For the construction of PKR2- $\Delta$ C52 mutant, we delete the region from 332 to 384, amplifying the region 1–331 by PCR with the R2 BamHI up and  $\Delta$ C tail EcoRI dw oligonucleotides using pcDNA-PKR2 as a template. The fragment digested with BamHI-EcoRI was inserted into pcDNA digested with the same enzymes (PKR2- $\Delta$ C52 pcDNA). We also constructed the PKR2- $\Delta$ I3 mutant in which we replaced the PKR2 sequence encoding region 262–384 with the fragment obtained by PCR corresponding to the region containing amino acids 272 to 384. PCR was performed using p426-R2 as a template and the oligonucleotides R2 EcoRI dw and  $\Delta$ I3 ApaI up, which were digested with EcoRI and ApaI and inserted into the p426-R2 digested with ApaI and EcoRI (PKR2- $\Delta$ I3p426). The insert obtained by digestion with EcoRI and BamHI was also ligated into pcDNA for transfection into the CHO cell line (PKR2- $\Delta$ I3pcDNA). For the BRET assay in mammalian culture cells, we amplified the PKR2 region from amino acid 1 to 362 by PCR with the oligonucleotides PKR2 NotI up and  $\Delta$ C BsiWI-dw, using pGAD-PKR2 as a template to obtain PKR2- $\Delta$ C52 rLuc. We amplified PKR2 cDNA by PCR with PKR2 NotI up and R2 BsiWI dw oligonucleotides, using R2- $\Delta$ I3p426 as a template to obtain PKR2- $\Delta$ I3 rLuc. The fragments digested with NotI-BsiWI were inserted into the

pRLuc-N vector (PerkinElmer) upstream of the Renilla luciferase cDNA and then transferred into a retroviral expression vector (pQC series, Clontech). Chimeric rGFP/ $\beta$ -arrestin-2 protein was obtained as described in [20]. For immunofluorescence localisation, we cloned the  $\beta$ -arrestin-2 cDNA in frame with GFP venus in pCMV. For GST pull-down assays, the proteins were expressed in *E. coli*. The CT-GST protein was obtained by fusing the 52 amino acids of the carboxyl terminus of PKR2 with GST. The C-terminal PKR2 region was amplified by PCR with R2CT BamHI up and R2 EcoRI dw and inserted into the pGEX vector (CT pGEX).  $\beta$ -arrestin-2 cDNA was amplified by PCR with gene-specific primers  $\beta$ -arrestin BamHI up and  $\beta$ -arrestin EcoRI dw and cloned into pBluescript ( $\beta$ -arrestin-2 pBS).  $\beta$ -Arrestin-2 p44 cDNA obtained by PCR using the oligonucleotides  $\beta$ -arrestin BamHI up and  $\beta$ -arrestin-p44 EcoRI dw was cloned into pBluescript (p44 pBS). The resulting plasmids,  $\beta$ -arrestin-2 pBS and p44 pBS, were digested with BamHI and EcoRI, and the resulting fragments were cloned into pET 28a ( $\beta$ -arrestin pET28 and p44 pET28) to express the recombinant proteins fused with a poly-his tag. For the cross-linking experiments, the  $\beta$ -arrestin-2 cDNA was also cloned into pCMV digested with BamHI and EcoRI to express the recombinant protein fused with a FLAG tag sequence ( $\beta$ -arrestin-2 pCMV). All oligonucleotides used for the plasmid constructions are listed in Table 1.

### 2.3. Preparation of yeast membrane and western blot analysis

Yeast cell membranes were purified from a 1 liter overnight culture essentially as previously described [9,10]. Membrane preparations (10  $\mu$ g protein/sample) were mixed with an equal volume of 2 $\times$  concentrated Laemmli sample buffer (125 mM Tris-HCl, pH 6.8, 20% glycerol, 4% SDS and 0.01% bromophenol blue) and incubated for 30 min at 25°C. The proteins were separated on 10% SDS-polyacrylamide gels and transferred to nitrocellulose membranes by blotting.

### 2.4. Expression and purification of recombinant proteins in *E. coli*

BL21 *E. coli* cultures expressing recombinant proteins were grown at 37°C until an optical density of 600 nm (OD), corresponding to 0.6, was reached. The cultures were grown for a further 4 h at 28°C in the presence of isopropyl- $\beta$ -D-1-thiogalactopyranoside (IPTG) 0.1 mM.

$\beta$ -arrestin-2 and p-44 were purified using a His-tagged protein purification kit (Novagen, Darmstadt, Germany). The purified recombinant proteins were separated by SDS-PAGE and analysed by Western blotting.

### 2.5. Glutathione S-transferase (GST) pull-down

Following IPTG-induced expression in *E. coli*, CT-GST fusion protein was purified from cell extracts by affinity chromatography using Glutathione Sepharose beads (GE Healthcare, Hatfield, UK) according to

**Table 1**  
Oligonucleotides used in the study.

Oligonucleotide	Sequence
R2 BamHI up	5'-AAGGATCCATGGCAGCCAGAAATGG-3'
$\Delta$ C tail EcoRI dw	5'-TTGAATTCATGGTGTGTCTTGACCG-3'
R2 EcoRI dw	5'-TTGAATTCCTCAGCGGTGATACAGTCC-3'
$\Delta$ I3 ApaI up	5'-GTGGGCCCTGTGGTCCACATGACC-3'
PKR2 NotI up	5'-
R2 BsiWI dw	AAAGCGCCGCCACCATGGCAGCCAGAAATGGAAACACC-3'
R2 $\Delta$ C BsiWI dw	5'-AAACGTACGCTTCAGGGTGATACAGTCCAC-3'
R2CT BamHI up	5'-AACGTACGCATGGTGTGTCTTGACCG-3'
$\beta$ -arrestin BamHI up	5'-GGATCCTGCTCGTGAACGGTCAAGAACAACACC-3'
$\beta$ -arrestin BamHI up	5'-AAGGATCCATGGGGGAGAAACCCGGG-3'
$\beta$ -arrestin EcoRI dw	5'-TTGAATTCGAGATTGATCATAGTCG-3'
$\beta$ -arrestin p44 EcoRI dw	5'-AGAATTCAGCGGCTGACTGGGTCTGGGG-3'

the manufacturer's instructions. In brief, 50  $\mu$ l slurry of glutathione-Sepharose beads equilibrated in buffer A (PBS, 1% Nonidet P 40, 1 mM EDTA, supplemented with protease inhibitor) was incubated with 2 ml CT-GST lysate for 1 h at 4°C with constant stirring. Beads with bound CT-GST were collected by centrifugation, washed extensively in buffer A and incubated with purified  $\beta$ -arrestin-2 or with purified  $\beta$ -arrestin-2 p44 expressed in *E. coli*. The beads were washed as described above, and the bound proteins were eluted with GSH according to the GE Healthcare procedure and analysed by Western blotting (WB).

## 2.6. Cell cultures, transfection, and stimulation

CHO (Chinese Hamster Ovary) cells were plated at a density of  $4 \times 10^5$  per well in 6-well plates or at  $4 \times 10^4$  per well on poly-D-lysine coated coverslips in 24-well plates and allowed to grow until they reached 70–80% confluence. Cells were grown in Dulbecco's Modified Eagle Medium/Nutrient mixture F-12 Ham (DMEM/F12) supplemented with 100 U/ml penicillin/streptomycin, 10% foetal bovine serum (FBS) and 2 mM L-glutamine (Sigma-Aldrich, Milan, Italy) at 37°C and 5% CO<sub>2</sub>. Transient transfection with the plasmid PKR2 pcDNA and PKR2- $\Delta$ C52 pcDNA or with the plasmid PKR2 pcDNA and  $\beta$ -arrestin-GFP pcDNA was performed in the presence of Lipofectamine 2000 (Invitrogen Life Technologies, Milan, Italy) according to the manufacturer's instructions. In brief, cells were incubated with the Lipo-DNA complex for 24 h at 37°C and 5% CO<sub>2</sub>. A total of 24 h after transfection, cells were deprived of serum and stimulated with PK2 (100 nM) for 1 h at 37°C and 5% CO<sub>2</sub>. At the end of the incubation period, the cells cultured in 6-well plates were lysed in RIPA lysis buffer with a protease inhibitor cocktail (1% v/v) (Sigma Aldrich), quantified and used for WB analysis. Cells cultured on coverslips were fixed in 4% PFA (paraformaldehyde) for 10 min, washed 1  $\times$  in PBS and used for immunofluorescence analysis. PK2 was expressed and purified in *P. pastoris* as previously described [7].

Hek293 cell lines stably expressing each luminescent receptor in conjunction with the fluorescent  $\beta$ -arrestin-2 were obtained as follows. First, we prepared a cell line stably expressing the fluorescent acceptor rGFP/ $\beta$ -arrestin-2 by infecting the cells with a retroviral vector encoding for the corresponding cDNAs. Then we transduced the cells with luminescent receptor encoding vector either PKR2-rLuc or PKR2- $\Delta$ C52-rLuc or PKR2- $\Delta$ I3-rLuc. Stable co-expressing cell lines were selected by culturing cell populations in DMEM, 10% FBS added with the proper combination of antibiotics. The levels of luminescent receptors expressed in association with the fluorescent  $\beta$ -arrestin-2 in the stable co-expressing Hek293 cell lines were determined by measuring intrinsic luminescence in cell-membrane preparations as described in [19].

The clonal fibroblast lines isolated from mouse embryos carrying the targeted ablation of either  $\beta$ -arrestin-2 or both  $\beta$ -arrestin-1 and  $\beta$ -arrestin-2 ( $\beta$ -arr-2 KO-MEF and  $\beta$ -arr-1/2 KO-MEF cells) were made available to us by Prof. Robert J. Lefkowitz (Duke University, Durham, NC, USA).

MEF (mouse embryo fibroblast) wild-type,  $\beta$ -arr-2 KO-MEF and  $\beta$ -arr-1/2 KO-MEF cells were grown in a 6-well plate at a density of  $4 \times 10^5$  per well in DMEM medium supplemented with 100 U/mL penicillin/streptomycin, 10% FBS and 2 mM L-glutamine (Sigma-Aldrich, Milan, Italy) at 37°C and 5% CO<sub>2</sub>. Transient transfection with the plasmid PKR2 pcDNA and PKR2- $\Delta$ C52 pcDNA was performed in the presence of Lipofectamine 2000 (Invitrogen Life Technologies, Milan, Italy) according to the manufacturer's instructions. In brief, cells were incubated with the Lipo-DNA complex for 24 h at 37°C and 5% CO<sub>2</sub>. A total of 24 h after transfection, cells were deprived of serum and stimulated with PK2 (100 nM) for 5, 10, 30 and 60 min at 37°C and 5% CO<sub>2</sub>. At the end of the incubation period, the cells were lysed in RIPA lysis buffer with a protease inhibitor cocktail (1% v/v) (Sigma Aldrich), quantified and used for WB analysis.

## 2.7. Crosslinking

CHO cells were transiently transfected with  $\beta$ -arrestin pCMV and PKR2 pcDNA or PKR2- $\Delta$ C52 pcDNA to express FLAG-tagged  $\beta$ -arrestin-2 with wild-type (WT) PKR2 receptor or with PKR2- $\Delta$ C52 mutant. After transfection (24 h), cells were incubated with vehicle or 100 nM PK2 for 15 min at 37°C. The stimulations were stopped by adding the membrane-permeable cross-linker Dithiobis (succinimidyl propionate) (Sigma, Poole, Dorset, U.K.) at a final concentration of 2 mM. The cells were then incubated with gentle shaking at room temperature, washed twice with 50 mM Tris/HCl, pH 7.4, in PBS to neutralise unreacted dithiobis (succinimidyl propionate) and incubated in 0.5 ml 50 mM Hepes, pH 7.4, 50 mM NaCl, 10% (v/v) glycerol, 0.5% (v/v) Nonidet P40, 2 mM EDTA, 100  $\mu$ M Na<sub>3</sub>VO<sub>4</sub>, 1 mM PMSF, 10  $\mu$ g/ml benzamide, 5  $\mu$ g/ml soya bean trypsin inhibitor and 5  $\mu$ g/ml leupeptin and clarified by centrifugation (2 min at 153 g and 4°C). Aliquots (25  $\mu$ l) of whole cell lysates were collected and mixed with an equal volume of 2 $\times$  reducing loading buffer. The immunoprecipitates were washed 3 times with glycerol lysis buffer and eluted in 1 $\times$  reducing loading buffer for 15 min at 45°C.

## 2.8. Western blotting

After electrophoretic separation, the proteins were transferred to a nitrocellulose membrane (TCM) and blocked in 1% non-fat milk 1% BSA/Tris-buffered saline with 0.10% Tween-20 (TBS-T pH 7.4) for 1 h at room temperature. The membranes were then incubated overnight at 4°C with the appropriate primary antibody in the blocking solution. After extensive washing with TBS-T, the membranes were incubated with anti-mouse or anti-goat IgG, HRP-linked secondary antibodies for 1 h at room temperature. The immunoreactive signals were visualised using an enhanced chemiluminescence system. Quantification of signal intensity of Western blotting bands was performed using ImageJ software (<http://imagej.nih.gov/ij/index.html>) and relative protein expression was calculated after normalisation to the total protein of interest. Data were obtained from three separate experiments.

## 2.9. BRET assay

Receptor- $\beta$ -arrestin-2 interaction was measured on monolayers of stably co-expressing cells plated in white 96-well culture plates (Opti-Plate, Packard) using a plate luminometer (VICTOR light, PerkinElmer). Cell culture medium was replaced with 40  $\mu$ l PBS containing 5  $\mu$ M coelenterazine, 10 min before the addition of 10  $\mu$ l of 5 $\times$  concentrated ligand. Readings were recorded after 5 min of further incubation. The BRET ratio was determined as the ratio of high-energy (donor) and low-energy (acceptor) emissions recorded sequentially. The concentration-response curves were analysed by nonlinear curve fitting to the general logistic function:  $y = (a-d)/[1 + (x/c)^b] + d$ , where y and x are the BRET ratio and ligand concentration, a and d, are the upper and lower asymptotes, c is the ligand concentration causing the half-maximum BRET change, and b is the slope factor at c [19].

## 2.10. Immunofluorescence

CHO cells were washed in PBS 1 $\times$ , blocked for 1 h in 5% normal donkey serum and then incubated overnight at 4°C with a rabbit polyclonal antibody against PKR2 (Alomone Labs, Jerusalem, Israel). Cells were then washed with PBS 1 $\times$  and incubated for 1 h at room temperature with secondary anti-species IgG antibodies coupled to Alexa Fluor-555 (Immunological Sciences). The cell nuclei were stained with DAPI (Sigma Aldrich). The fluorescence signal was recorded using an Eclipse E600 fluorescence microscope (Nikon Instruments, Japan) connected to a QImaging camera with 64-bit NIS-Elements BR 3.2 software. The Pearson correlation coefficients were created using the ImageJ software (<http://imagej.nih.gov/ij/index.html>, free software) and the special

JACoP plug-in.

### 2.11. Data analysis

The data were plotted and analysed using GraphPad Prism 7 for Windows. All results were expressed as mean  $\pm$  SEM. Statistical analyses were performed using One-Way ANOVA followed by Dunnett's multiple comparisons post-test. Differences were considered significant at  $p < 0.05$ .

## 3. Results

### 3.1. Analysis of $\beta$ -arrestin-2 recruitment to the C-terminal tail of PKR2

Analysis of immunofluorescence experiments shows that, in the absence of PK2,  $\beta$ -arrestin-2 is predominantly localized inside the cells together with PKR2. Treatment with PK2 promotes the translocation of  $\beta$ -arrestin-2 with PKR2 in the plasmatic membrane (Fig. 1A). BRET utilizes bioluminescent and fluorescent protein tags with compatible emission and excitation properties, so that resonance energy transfer can be studied when the tags are in close proximity ( $< 10$  nm), which is a typical outcome of protein-protein interactions.

The BRET assay performed with Hek293 cells stably co-expressing

luminescent PKR2 (PKR2-rLuc) and fluorescent  $\beta$ -arrestin-2 (rGFP/ $\beta$ -arrestin-2) shows that activation of PKR2 leads to a concentration-dependent increase in  $\beta$ -arrestin-2 recruitment (Fig. 1B).

The value of the BRET ratio observed in the absence of PK2 ligand (basal) is consistent with the constitutive association between PKR2 and  $\beta$ -arrestin-2 (Fig. 1B), as previously shown by Sbai et al. [20].

To test the importance of the C-terminal tail in modulating  $\beta$ -arrestin-2 recruitment, we examined the interaction of the PKR2- $\Delta$ C52 mutant (Fig. 1C) and  $\beta$ -arrestin-2 in Hek293 cells stably co-expressing the PKR2- $\Delta$ C52 and rGFP/ $\beta$ -arrestin-2 proteins. As shown in Fig. 1B, PK2 was no longer able to trigger the recruitment of  $\beta$ -arrestin-2 to the PKR2- $\Delta$ C52 mutant. However, the ability of PKR2- $\Delta$ C52 to constitutively associate with  $\beta$ -arrestin-2 in the absence of the agonist persisted, and was even slightly increased, although the expression level of the mutant receptor (measured as described in the Methods section) was significantly lower compared to wild type (PKR2- $\Delta$ C52 = 1.7).

To further investigate physical interaction between  $\beta$ -arrestin-2 and PKR2, we expressed WT PKR2 or the mutant PKR2- $\Delta$ C52 receptor together with  $\beta$ -arrestin-2 in CHO cells, we analysed the binding of WT PKR2 and PKR2- $\Delta$ C52 mutant receptors to  $\beta$ -arrestin-2 by cross-linking experiments. We first verified that the expression levels of PKR2- $\Delta$ C52 mutant and WT PKR2 in CHO were comparable (Fig. 2A). Then, cells were incubated with the cross-linker, irradiated with UV light and the

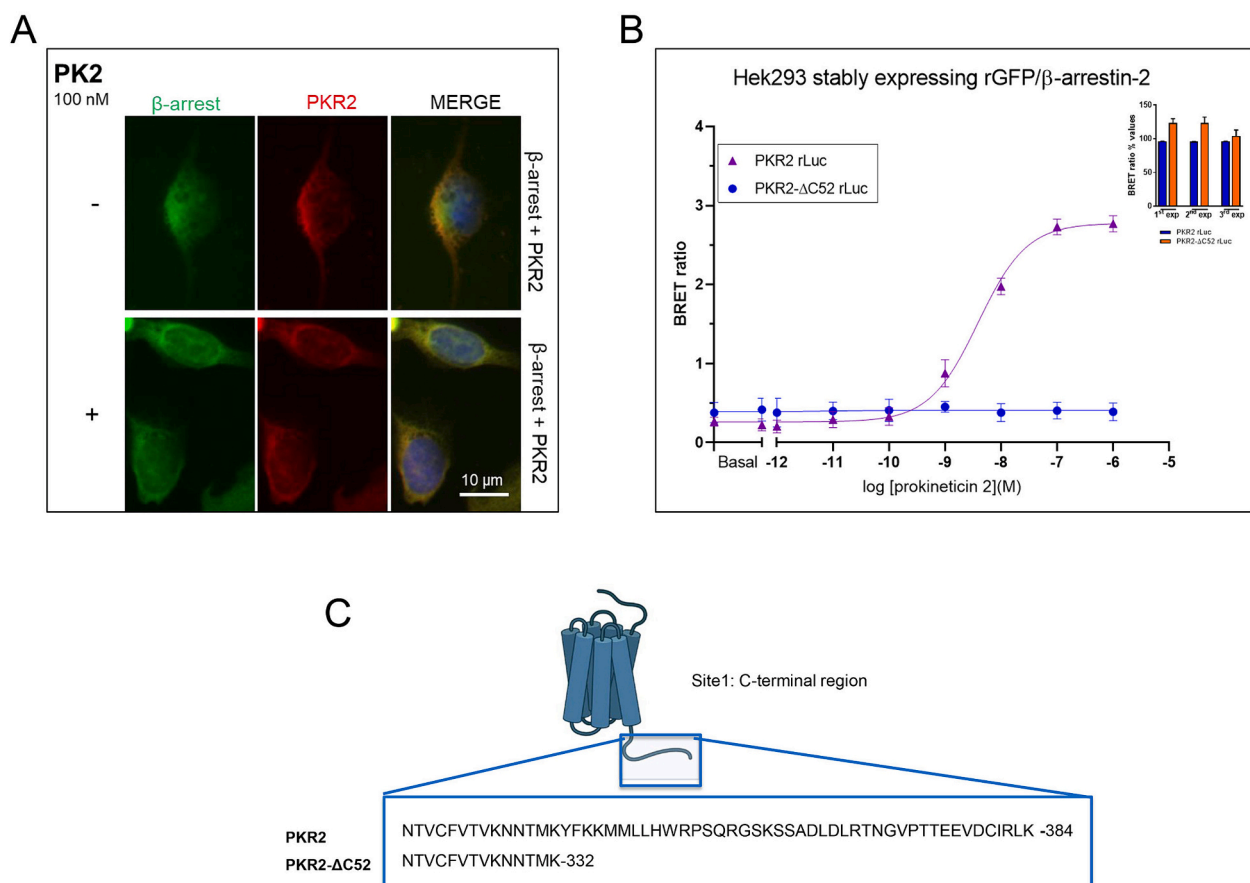


**Fig. 1.** WT PKR2 and PKR2- $\Delta$ C52 receptor mutant interaction with  $\beta$ -arrestin-2. (A) Representative immunofluorescence images of CHO cells transfected with rGFP/ $\beta$ -arrestin-2 (green) and PKR2 (red) in the absence of PK2 (-) or in the presence of PK2 100 nM (+) for 1 h. Scale bar 10  $\mu$ m. The cell nuclei were counterstained with DAPI (blue). (B) Concentration-response curves for PK2 recorded by BRET assay in Hek293 cells stably co-expressing either PKR2-rLuc or PKR2- $\Delta$ C52-rLuc in conjunction with rGFP/ $\beta$ -arrestin-2. Two independent experiments were conducted with similar results and in each of them, the sample measurements were performed in triplicate. Data (symbols) are the mean  $\pm$  SEM of triplicate determinations obtained in one representative experiment and are shown with the best-fitting theoretical curves (solid line). The histogram (insert) represents three independent experiments made in triplicate. Data are expressed as a percentage of the PKR2- $\beta$ -arrestin-2 interaction signal measured in the absence of ligand (100%) and are the mean  $\pm$  SEM of triplicate determinations carried out in each experiment. (C) Schematic representation of the WT PKR2 receptor and the PKR2- $\Delta$ C52 mutant. (For interpretation of the references to colour in this figure legend, the reader is referred to the web version of this article.)

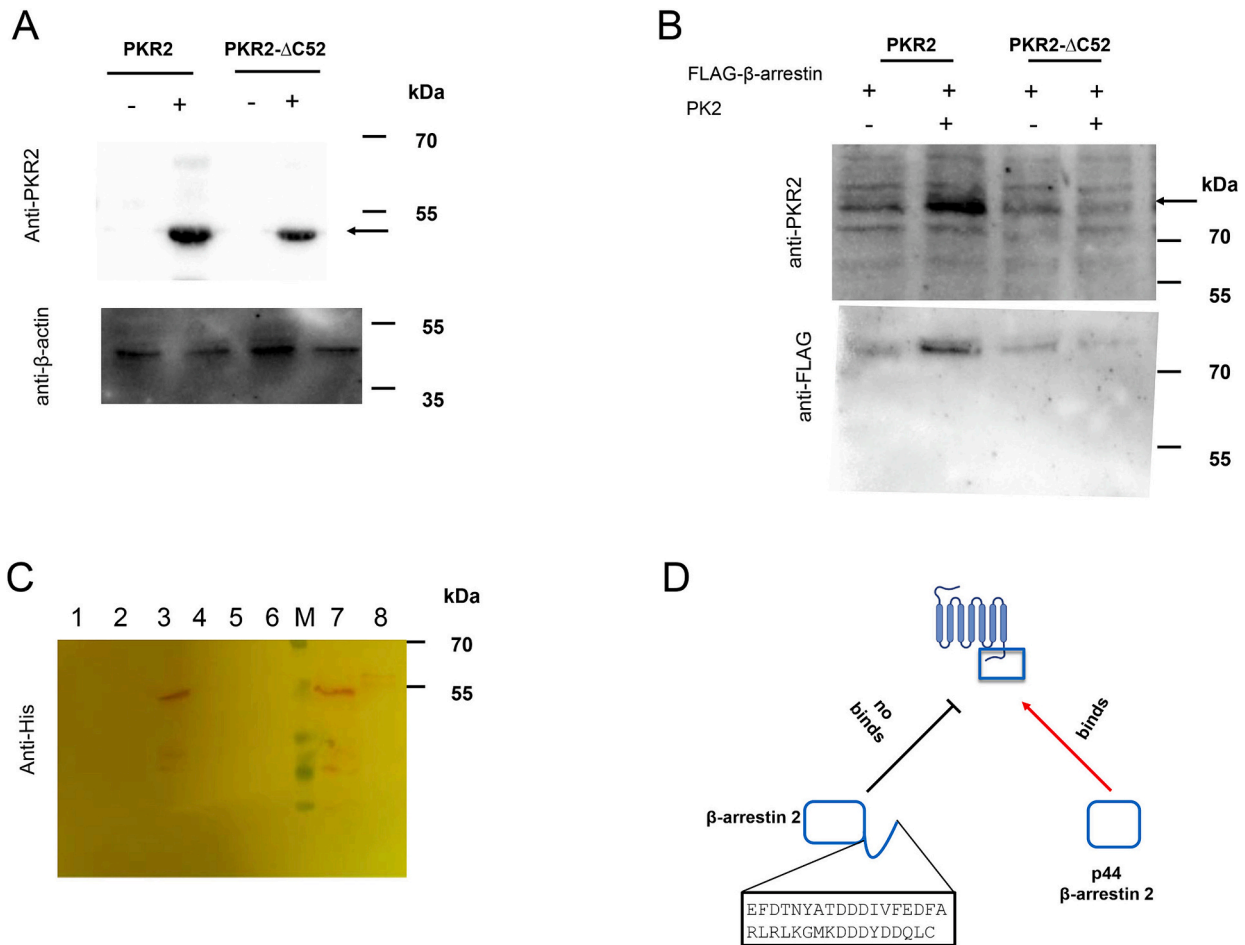


**Fig. 2.** Interaction of  $\beta$ -arrestin-2 with the C-terminal region of PKR2. (A) Expression of WT PKR2 and the PKR2- $\Delta$ C52 receptor mutant in CHO cells. The arrow indicates the position of WT PKR2 or the PKR2- $\Delta$ C52 mutant. (B) Cross-linking of  $\beta$ -arrestin-2 with WT PKR2 or the mutant PKR2- $\Delta$ C52 receptor. CHO cells expressing WT PKR2 or the PKR2- $\Delta$ C52 mutant and  $\beta$ -arrestin-2 with FLAG tag were incubated with succinimidyl propionate. The proteins were immunoblotted and analysed with anti-PKR2 and anti-FLAG antibodies. The arrow indicates the position of the complex of WT PKR2 or the PKR2- $\Delta$ C52 mutant with  $\beta$ -arrestin-2. (C) The GST-fusion protein CT-GST was used to pull down  $\beta$ -arrestin-2 or  $\beta$ -arrestin-2 p44, and the resulting elution solutions were resolved on 12% SDS-PAGE and analysed with an anti-His antibody by Western blotting. Lane 1/2:  $\beta$ -arrestin-2 p44 wash solution; lane 3:  $\beta$ -arrestin-2 p44 eluate; lane 4/5:  $\beta$ -arrestin-2 wash solution; lane 6:  $\beta$ -arrestin-2 eluate; lane 7:  $\beta$ -arrestin-2 p44 input; lane 8:  $\beta$ -arrestin-2 input. (D). Schematic representation of the results of the GST pull-down experiment.

membrane proteins were fractionated by SDS-PAGE, blotted, and then analysed with the PKR2 antibody (Fig. 2B). The results show that the constitutive association between WT PKR2 receptor and  $\beta$ -arrestin-2 was significantly increased in the presence of a PK2 agonist.

The C-terminally truncated receptor, PKR2- $\Delta$ C52, can also be co-precipitated with  $\beta$ -arrestin-2 in the absence of ligand, however, the addition of PK2 does not result in the increase of the interaction signal (Fig. 2B).

To confirm the interaction between the C-terminal region of PKR2 and  $\beta$ -arrestin-2, the C-terminal region of PKR2 was expressed in bacteria as a GST fusion protein (PKR2CT-GST).  $\beta$ -arrestin-2 and  $\beta$ -arrestin-2 p44 were expressed in *E. coli* and fused to His Tag. The  $\beta$ -arrestin-2 p44 mutant, was obtained by deleting the  $\beta$ -arrestin-2-tail region of 35 amino acids and was designated as  $\beta$ -arrestin-2 p44, because comprising the same amino acid sequence of p44 splice variant of visual arrestin [22]. The PKR2CT-GST fusion protein was purified on glutathione agarose and then used in direct binding experiments with  $\beta$ -arrestin-2 and  $\beta$ -arrestin-2 p44 (Fig. 2C).  $\beta$ -arrestin-2 does not bind to PKR2CT-GST, but  $\beta$ -arrestin-2 p44 is able to bind to PKR2CT-GST (Fig. 2C). Parallel control experiments show that neither  $\beta$ -arrestin-2 nor  $\beta$ -arrestin-2 p44 mutant bound to GST alone (data not shown). The result of the GST pull-down experiment is shown schematically in Fig. 2D.

The results are consistent with previous studies showing that p44

visual arrestin binds the non-phosphorylated C-terminal tail of the rhodopsin receptor stronger than visual arrestin [22] and that the truncated  $\beta$ -arrestin-1 mutant binds more efficiently to the neurotensin-1 receptor compared to  $\beta$ -arrestin-1 [23].

### 3.2. Analysis of $\beta$ -arrestin-2 recruitment to the core region of PKR2: Role of the intracellular receptor loop 3

To determine the role of intracellular receptor loop 3 (ICL3) in the interaction between PKR2 and  $\beta$ -arrestin-2, we constructed a mutant by deleting a central sequence extending from amino acid 262 to 272 of the ICL3 loop (Fig. 3A). First, we found that the expression level of the mutant PKR2- $\Delta$ I3 and WT PKR2 in CHO was comparable (Fig. 3B). We then analysed the binding of the mutant PKR2- $\Delta$ I3 receptor to  $\beta$ -arrestin-2 by cross-linking experiments. The cells were incubated with the cross-linker, irradiated with UV light and the membrane proteins were fractionated by SDS-PAGE, blotted, and then probed with the anti-PKR2 antibody and the anti-FLAG antibody. The results show that the PKR2- $\Delta$ I3 mutant is unable to bind  $\beta$ -arrestin-2 both in the presence and absence of PK2 agonist (Fig. 3C).

The mutant receptor fused to rLuc (PKR2- $\Delta$ I3 rLuc) was then co-expressed in the Hek293 cell line stably expressing the fluorescent form of  $\beta$ -arrestin-2 (rGFP/ $\beta$ -arrestin-2). The level of PKR2- $\Delta$ I3 rLuc

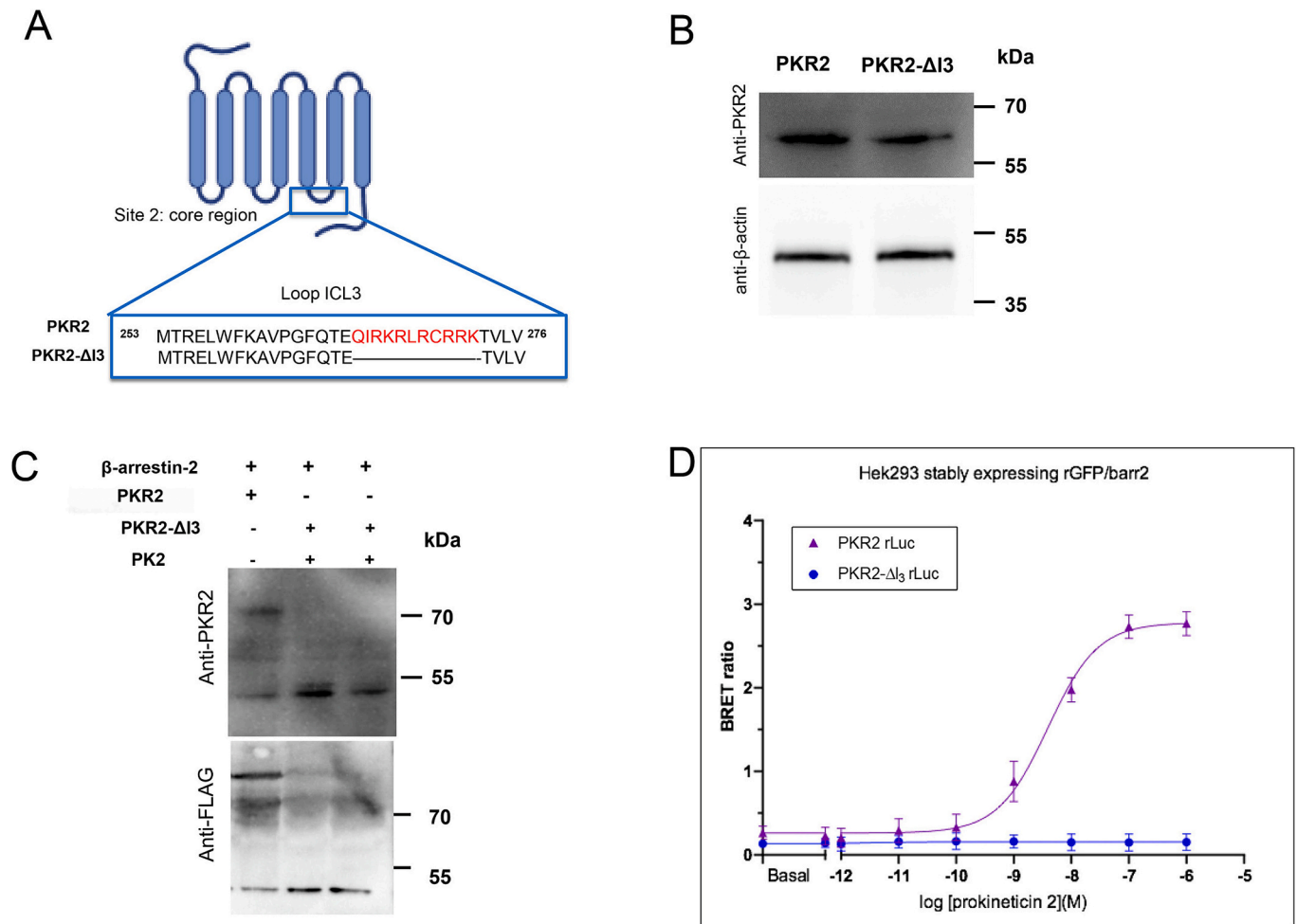


**Fig. 3.** Interaction of  $\beta$ -arrestin-2 with the ICL3 region of PKR2. (A) Schematic representation of the WT PKR2 receptor and the PKR2- $\Delta$ I3 mutant. (B) Expression of WT PKR2 and the PKR2- $\Delta$ I3-rLuc receptor mutant in CHO cells. (C) Cross-linking of  $\beta$ -arrestin-2 with WT PKR2 or the mutant PKR2- $\Delta$ I3 receptor. CHO cells expressing WT PKR2 or the PKR2- $\Delta$ I3 mutant and  $\beta$ -arrestin-2-FLAG were incubated with succinimidyl propionate. Proteins were immunoblotted and analysed with anti-PKR2 and anti-FLAG antibodies. (D) BRET signal induced by increasing concentrations of PK2. BRET assay was performed in Hek293 stably co-expressing rGFP/ $\beta$ -arrestin-2 in association with either PKR2-rLuc or PKR2- $\Delta$ I3-rLuc. Two independent experiments were conducted with similar results and in each of them, the sample measurements were performed in triplicate. Data (symbols) represent the mean  $\pm$  SEM of triplicate determinations obtained in one representative experiment and are plotted with the best-fit theoretical curves (solid lines) calculated as described in Methods.

receptor expression was comparable to that of WT PKR2 (PKR2/ PKR2- $\Delta$ I3 ratio = 1.2, data not shown).

The BRET assay shows that deletion of ICL3 results in loss of the receptor's ability to interact with  $\beta$ -arrestin-2. This suggests that ICL3 is a necessary region that allows receptor to interact with  $\beta$ -arrestin-2 either in the absence or presence of the PK2 agonist ligand (Fig. 3D).

### 3.3. PKR2- $\beta$ -arrestin-2 mediated signalling

It is known that  $\beta$ -arrestin not only desensitises GPCR signalling but also initiates  $\beta$ -arrestin-dependent signalling via ERK<sub>1/2</sub>, which leads to the subsequent phosphorylation and activation of target proteins such as protein kinases, transcription factors and membrane proteins, and regulates cell growth and differentiation [24–26].

After PK2 stimulation of mouse embryonic fibroblast cells (MEFs) transfected with PKR2, we analysed the time course of PK2-dependent ERK<sub>1/2</sub> phosphorylation. The results show that, following agonist addition, ERK phosphorylation (p-ER 1/2) starts to increase after 5 min, reaches the highest levels after 10 min, and remains detectable at longer time points (Fig. 4A). PK2 treatment of MEFs transfected with the PKR2- $\Delta$ C52 mutant results in significant ERK<sub>1/2</sub> activation at early time points after stimulation, with levels comparable to those detected in MEFs cells

transfected with PKR2. However, agonist stimulation does not lead to an increase in p-ERK<sub>1/2</sub> signal at later time points (Fig. 4B). To demonstrate that the activation of ERK at late time points is due to a general MAPK regulatory mechanism through  $\beta$ -arrestin-mediated GPCR crosstalk, we used MEFs cells lacking  $\beta$ -arrestin-2 ( $\beta$ -arr-2 KO) and MEFs cells lacking both  $\beta$ -arrestin-1 and  $\beta$ -arrestin-2 ( $\beta$ -arr-1/2 KO). In  $\beta$ -arr-2 KO MEFs cells transfected with PKR2, agonist induced ERK phosphorylation signal which significantly increases after 10 min but is no longer detectable after 60 min of stimulation (Fig. 4C). Similarly, PK2 stimulation of  $\beta$ -arr-1/2 KO MEF cells transfected with PKR2 induces ERK activation only after 10 min (Fig. 4D). In contrast, PK2 treatment of  $\beta$ -arr-1/2 KO MEF cells co-transfected with PKR2 and  $\beta$ -arrestin-2 induces a temporal ERK activation comparable to that observed in WT MEF cells transfected with PKR2 (Fig. 4E).

## 4. Discussion

The carboxyl-terminal tail of G protein-coupled receptors varies widely in both sequence and length and appears to be essential for G-protein coupling and GPCR trafficking [1]. Receptor C-terminal region also serves as a docking site for regulatory proteins, such as those of the  $\beta$ -arrestin family [27–29]. GPCRs have two binding sites for  $\beta$ -arrestins.

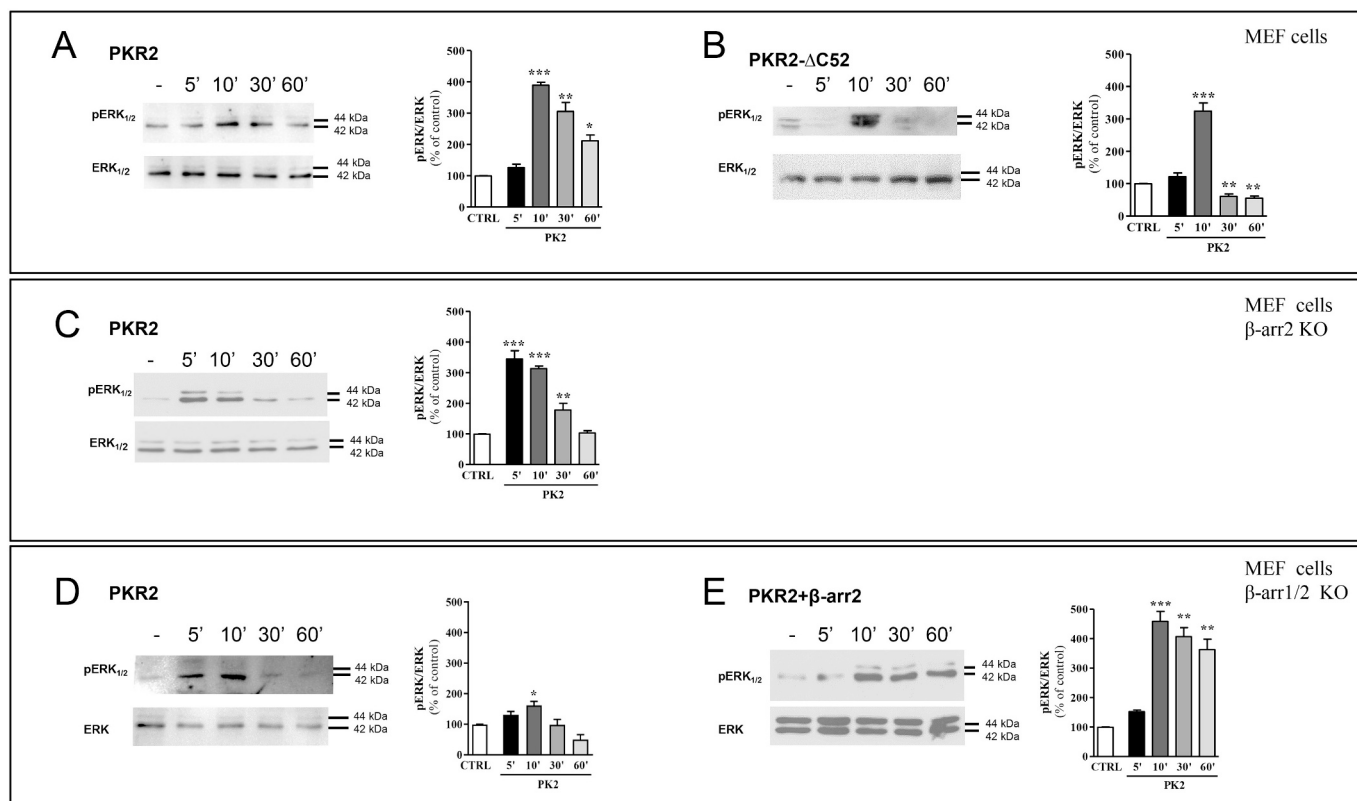


**Fig. 4.** PK2-dependent temporal ERK activation. Analysis of ERK<sub>1/2</sub> phosphorylation in wild type MEF cells transfected with (A) WT PKR2 and (B) the PKR2-ΔC52 mutant. Analysis of ERK<sub>1/2</sub> phosphorylation in β-arr-2 KO-MEF cells with (C) WT PKR2. Analysis of ERK<sub>1/2</sub> phosphorylation in β-arr-1/2 KO-MEF cells transfected with (D) WT PKR2 and (E) WT PKR2 and β-arrestin-2. The densitometric plots show pERK<sub>1/2</sub> and ERK<sub>1/2</sub> protein levels after 5, 10, 30, and 60 min after treatment with PK2 100 nM, respectively. The bar graphs show the ratio of pERK<sub>1/2</sub>/ERK<sub>1/2</sub> and the percentage increase compared to unstimulated cells (CTRL). The bars show the mean values ± SEM from the three experimental conditions. A one way-ANOVA was used for statistical analysis followed by a Dunnett's test for multiple comparisons \*\*  $p < 0.01$ , \*\*\*  $p < 0.001$ .

The first interaction site, known as the “tail interaction”, occurs between the cytosolic tail of a GPCR and the N-terminal domain of β-arrestin, allowing its active conformation. The second site consists of cytoplasmic GPCR loops, in particular intracellular loop 3, which, after ligand binding and outward movement of helix V and VI, form a cavity in the transmembrane bundle that interacts with central β-arrestin ridge. This interaction known as the “core interaction”, occupies a similar binding domain to the α-subunit of the G protein, resulting in direct competition between β-arrestin and G proteins in binding the active GPCRs [2].

The stability of the GPCR-β-arrestin interaction depends on the affinity of β-arrestin for the GPCR, which is strongly influenced by the C-terminal sequence of the GPCR, in particular by the presence or absence of cluster of phosphorylation sites [30]. Depending on the temporal stability of the β-arrestin interaction, GPCRs are categorised into type A and type B [2]. Several results indicate that PKR2 is a type A GPCR since it preferentially interacts with β-arrestin-2 [19,28]. This is due to the specific set of phosphorylation sites present in the C-terminal region of PKR2 [19,20,28].

Analysis of β-arrestin-2- PKR2 interaction by BRET assay shows a degree of β-arrestin-2-receptor interaction in the absence of ligand that is enhanced by the addition of agonist, in a concentration-dependent manner [20]. It is tempting to hypothesize that this constitutive binding may be largely due to β-arrestin-PKR2 interactions within intracellular compartments. Indeed, in the absence of a ligand, the BRET experiment cannot distinguish between cell surface receptors and intracellular receptors. In several cell types, PKR2 mainly localized in the plasma membrane, has also been detected in the Golgi apparatus and the endoplasmic reticulum [20].

We have shown by BRET experiments that PK2 treatment cannot

increase the binding of β-arrestin-2 to the PKR2-ΔC52 mutant, although the interaction with β-arrestin-2 is conserved in the absence of the PK2 ligand. These results suggest that the C-terminal region of PKR2 is not critical for the binding of β-arrestin-2 to the unstimulated receptor. To confirm these results, we performed cross-linking experiments by transfecting β-arrestin-2 into CHO cells stably expressing WT PKR2 or the PKR2-ΔC52 mutant. The results show that WT PKR2-β-arrestin-2 interaction increase in the presence of the PK2 ligand, whereas the PKR2-ΔC52 binds β-arrestin-2 in a weakened form that is not affected by the presence of the PK2 ligand.

To investigate whether the binding of β-arrestin-2 to the PKR2 CT region is independent of the phosphorylation status of the receptor, we performed GST pull-down experiments with a chimeric protein obtained by fusing GST to the CT-terminal region of PKR2 (PKR2CT-GST). We examined the binding of PKR2CT-GST to β-arrestin-2 and β-arrestin-2 p44, a truncated mutant corresponding to p44 constitutively active splice variant of visual arrestin [22,31] and β-arrestin-1 truncated mutant [23]. The results show that β-arrestin-2 p44 binds to the non-phosphorylated CT-terminal region of PKR2, whereas β-arrestin-2 does not bind to the CT-terminal region. To analyse the role β-arrestins-1 and 2 in ERK activation, a time course of ERK activation after treatment with PK2 ligand was performed in MEFs β-arrestin-2 KO, β-arrestin-1 and 2 double KO, and β-arrestin-1 and 2 double KO with reconstituted WT β-arrestin-2 transfected with PKR2. PK2 was shown to induce β-arrestin-2 mediated ERK activation after 60 min.

To analyse the interaction of β-arrestin-2 with the PKR2 core, we focus on the PKR2 mutant lacking the central ICL3 region. Previous studies have shown that ICL3 plays a crucial role in the interaction with G-proteins and in the localisation of PKR2 to the cell membrane [32].

Zhou's group identified two critical regions in ICL3, a proximal region comprising arginine-264, lysine-265 and arginine-266 (RKR), and the distal region extending from amino acids 270 to 274. Our results suggest that this part of ICL3, as in other GPCRs including rhodopsin, adrenergic and hormone/choriogonadotropin (LH/CG) receptors [2], also contributes to the binding of  $\beta$ -arrestin-2.

In BRET experiments performed on PKR2- $\Delta$ I3  $\beta$ -arrestin-2 stable co-expressing cells, PKR2- $\Delta$ I3 mutant is unable to bind  $\beta$ -arrestin-2 both in the presence or absence of PK2 suggesting that receptor C-tail alone is not sufficient for  $\beta$ -arrestin-2 to bind receptor neither at the plasma membrane nor at endoplasmic reticulum level. Therefore, this study provides insights into the molecular determinants that govern the formation of the prokineticin receptor-arrestin complex, particularly with regard to the role of the C-terminal tail and ICL3. Our data show that  $\beta$ -arrestin-2 is able to constitutively bind the PKR2 and that this basal binding is mediated by the core region, whereas it is not affected by the presence of the C-terminal region. Indeed, the PKR2- $\Delta$ C52 mutant is able to bind  $\beta$ -arrestin-2 in the absence of ligands, unlike the PKR2- $\Delta$ I3 mutant. On the contrary, agonist induced receptor activation is necessary for  $\beta$ -arrestin-2 to bind the C-terminus, and in turn adopt a conformation suitable to trigger intracellular signalling, ultimately leading to the activation of ERK. It is possible to speculate that  $\beta$ -arrestin-2 binds sequentially to PKR2, or rather as that a first binding to the core, basal interaction, is required for subsequent agonist mediated binding to the C-terminal region.

## 5. Conclusions

Understanding how GPCRs recruit and maintain interactions with  $\beta$ -arrestins should drive the development of better functionally selective therapeutics and clarify important questions related to receptor expression and the ligand pharmacology.

## Author contributions

R.L. and R.M. were responsible for the overall conception of the project, planned the experiments and supervised, edited and contributed to the critical revision of the manuscript. I.C., M.R.F., M.V. and D.M. conducted the experiments and analysed the data. All authors have read and approved the published version of the manuscript.

## Funding

This work was supported by grants from Sapienza, University of Rome and by Fondazione Sovena, Rome, Italy (fellowship to Vincenzi M.).

## CRediT authorship contribution statement

**R. Lattanzi:** Writing – review & editing, Supervision, Project administration, Funding acquisition, Data curation, Conceptualization. **I. Casella:** Writing – original draft, Software, Methodology, Investigation, Formal analysis, Data curation. **M. Vincenzi:** Writing – original draft, Software, Methodology, Investigation, Data curation. **D. Maftai:** Writing – original draft, Visualization, Software, Methodology, Investigation, Data curation. **R. Miele:** Writing – review & editing, Visualization, Supervision, Funding acquisition, Data curation, Conceptualization.

## Declaration of competing interest

The authors declare that they have no known competing financial interests or personal relationships that could have appeared to influence the work reported in this paper.

## Data availability

The data presented in this study are available on request from the corresponding author.

## References

- [1] D.M.F. Rosenbaum, S.G.F. Rasmussen, B.K. Kobilka, The structure and function of G-protein-coupled receptors, *Nature* 459 (2009) 356–363, <https://doi.org/10.1038/nature08144>.
- [2] M. Seyedabadi, M. Gharghabi, V. Gurevich, V. Vsevolod, The GPCR perspective, *Biomolecules* 11 (2021) 218, <https://doi.org/10.3390/biom11020218>.
- [3] V.V. Gurevich, E.V. Gurevich, The structural basis of arrestin-mediated regulation of G-protein-coupled receptors, *Pharmacol. Ther.* 110 (2006) 465–502, <https://doi.org/10.1016/j.pharmthera.2005.09.008>.
- [4] R. Lattanzi, R. Miele, Prokineticin-receptor network: mechanisms of regulation, *Life* 12 (2022) 172, <https://doi.org/10.3390/life12020172>.
- [5] R. Lattanzi, D. Maftai, M.R. Fullone, R. Miele, Trypanosoma cruzi trans-sialidase induces STAT3 and ERK activation by prokineticin receptor 2 binding, *Cell Biochem. Funct.* 39 (2021) 326–334, <https://doi.org/10.1002/cbf.3586>.
- [6] J. Chen, C. Kuei, S. Sutton, S. Wilson, J. Yu, F. Kamme, C. Mazur, T. Lovenberg, C. Liu, Identification and pharmacological characterization of prokineticin 2 beta as a selective ligand for prokineticin receptor 1, *Mol. Pharmacol.* 67 (2005) 2070–2076, <https://doi.org/10.1124/mol.105.011619>.
- [7] R. Lattanzi, D. Maftai, L. Negri, I. Fusco, R. Miele, PK2 $\beta$  ligand, a splice variant of prokineticin 2, is able to modulate and drive signaling through PKR1 receptor, *Neuropeptides* 71 (2018) 32–42.
- [8] R. Lattanzi, D. Maftai, M. Vincenzi, M.R. Fullone, R. Miele, Identification and characterization of a new splicing variant of Prokineticin 2, *Life* 12 (2022) 248, <https://doi.org/10.3390/life12020248>.
- [9] R. Lattanzi, D. Maftai, M.R. Fullone, R. Miele, Identification and characterization of Prokineticin receptor 2 splicing TM4-7 variant and its modulation in an animal model of Alzheimer's disease, *Neuropeptides* 73 (2019) 49–56, <https://doi.org/10.1016/j.npep.2018.11.006>.
- [10] A.L. Chaly, D. Srisai, E.E. Gardner, J.A. Sebag, The Melanocortin receptor accessory protein 2 promotes food intake through inhibition of the Prokineticin Receptor-1, *eLife* 5 (2016) e12397, <https://doi.org/10.7554/eLife.12397>.
- [11] M.R. Fullone, D. Maftai, M. Vincenzi, R. Lattanzi, R. Miele, Identification of regions involved in the physical interaction between Melanocortin receptor accessory protein 2 and Prokineticin receptor 2, *Biomolecules* 12 (2022) 474, <https://doi.org/10.3390/biom12030474>.
- [12] M.R. Fullone, D. Maftai, M. Vincenzi, R. Lattanzi, R. Miele, Arginine 125 is an essential residue for the function of MRAP2, *Int. J. Mol. Sci.* 23 (2022) 9853, <https://doi.org/10.3390/ijms23179853>.
- [13] L. Negri, N. Ferrara, The Prokineticins: neuromodulators and mediators of inflammation and myeloid cell-dependent. *Angiogenesis, Physiol. Rev.* 98 (2018) 1055–1082, <https://doi.org/10.1152/physrev.00012.2017>.
- [14] J.V. Gardiner, A. Bataveljic, N.A. Patel, G.A. Bewick, D. Roy, D. Campbell, H. C. Greenwood, K.G. Murphy, S. Hameed, P.H. Jethwa, et al., Prokineticin 2 is a hypothalamic neuropeptide that potently inhibits food intake, *Diabetes* 59 (2010) 397–406, <https://doi.org/10.2337/db09-1198>.
- [15] D. Maftai, R. Lattanzi, M. Vincenzi, S. Squillace, M.R. Fullone, R. Miele, The balance of concentration between Prokineticin 2 $\beta$  and Prokineticin 2 modulates the food intake by STAT3 signaling, *BBA Adv.* 1 (2021) 100028, <https://doi.org/10.1016/j.bbadv.2021.100028>.
- [16] R. Lattanzi, R. Miele, Versatile role of Prokineticins and Prokineticin receptors in Neuroinflammation, *Biomedicines* 9 (2021) 1648, <https://doi.org/10.3390/biomedicines9111648>.
- [17] R. Lattanzi, C. Severini, R. Miele, Prokineticin 2 in cancer-related inflammation, *Cancer Lett.* 546 (2022) 215838, <https://doi.org/10.1016/j.canlet.2022.215838>.
- [18] R. Lattanzi, R. Miele, Non-peptide agonists and antagonists of the Prokineticin receptors, *Curr. Issues Mol. Biol.* 44 (2022) 6323–6332, <https://doi.org/10.3390/cimb44120431>.
- [19] I. Casella, C. Ambrosio, Prokineticin receptors interact unselectively with several G protein subtypes but bind selectively to  $\beta$ -arrestin 2, *Cell. Signal.* 83 (2021) 110000, <https://doi.org/10.1016/j.cellsig.2021.110000>.
- [20] Q. Sbai, C. Monnier, C. Dodé, J.P. Pin, J.P. Hardelin, P. Rondard, Biased signaling through G-protein-coupled PROKR2 receptors harboring missense mutations, *FASEB J.* 28 (2014) 3734–3744, <https://doi.org/10.1096/fj.13-243402>.
- [21] W. Yin, H. Liu, Z. Peng, D. Chen, J. Li, J.D. Li, Mechanisms that underlie the internalization and extracellular signal regulated kinase 1/2 activation by PKR2 receptor, *Cell. Signal.* 26 (2014) 1118–1124, <https://doi.org/10.1016/j.cellsig.2014.01.031>.
- [22] A. Pulvermuller, D. Maretzki, M. Rudnicka-Nawrot, W.C. Smith, K. Palczewski, K. P. Hofmann, Functional differences in the interaction of Arrestin and its splice variant, p44, with rhodopsin, *Biochemistry* 36 (1997) 9253–9260, <https://doi.org/10.1021/bi970772g>.
- [23] W. Huang, M. Masureel, Q. Qu, J. Janetzko, A. Inoue, H.E. Kato, M.J. Robertson, K. C. Nguyen, J.S. Glenn, G. Skiniotis, B.K. Kobilka, Structure of the neurotensin receptor 1 in complex with  $\beta$ -arrestin 1, *Nature* 579 (2020) 303–308.
- [24] L.M. Luttrell, R.J. Lefkowitz, The role of  $\beta$ -arrestins in the termination and transduction of G-protein-coupled receptor signals, *J. Cell Sci.* 115 (2002) 455–465.



- [25] S.K. Shenoy, J. Lefkowitz,  $\beta$ -Arrestin-mediated receptor trafficking and signal transduction, *Trends Pharmacol. Sci.* 32 (2011) 521–533.
- [26] Y.K. Peterson, L.M. Luttrell, The diverse roles of arrestin scaffolds in G protein-coupled receptor signaling, *Pharmacol. Rev.* 69 (2017) 256–297, <https://doi.org/10.1124/pr.116.013367>.
- [27] R.H. Oakley, S.A. Laporte, J.A. Holt, M.G. Caron, L.S. Barak, Differential affinities of visual arrestin,  $\beta$ arrestin1, and  $\beta$ arrestin2 for G protein-coupled receptors delineate two major classes of receptors, *J. Biol. Chem.* 275 (2000) 17201–17210, <https://doi.org/10.1074/jbc.M910348199>.
- [28] X.E. Zhou, Y. He, P.W. de Waal, X. Gao, Y. Kang, N. Van Eps, Y. Yin, K. Pal, D. Goswami, T.A. White, A. Barty, N.R. Latorraca, H.N. Chapman, W.L. Hubbell, R. O. Dror, R.C. Stevens, V. Cherezov, V.V. Gurevich, P.R. Griffin, O.P. Ernst, K. Melcher, H.E. Xu, Identification of phosphorylation codes for arrestin recruitment by G protein-coupled receptors, *Cell* 170 (2017) 457–469.e13, <https://doi.org/10.1016/j.cell.2017.07.002>.
- [29] E. Pottier, J. Storme, C.P. Stove, The P2Y2 receptor C-terminal tail modulates but is dispensable for  $\beta$ -Arrestin recruitment, *Int. J. Mol. Sci.* 23 (2022) 3460, <https://doi.org/10.3390/ijms23073460>.
- [30] E. Ghosh, H. Dwivedi, M. Baidya, A. Srivastava, P. Kumari, T. Stepniewski, H. R. Kim, M.-H. Lee, J. van Gastel, M. Chaturvedi, D. Roy, S. Pandey, J. Maharana, R. Guixà-González, L.M. Luttrell, K.-Y. Chung, S. Dutta, J. Selent, A.K. Shukla, Conformational sensors and domain swapping reveal structural and functional differences between  $\beta$ -Arrestin isoforms, *Cell Rep.* 28 (2019) 3287–3299. e6, <https://doi.org/10.1016/j.celrep.2019.08.053>.
- [31] N.R. Latorraca, J.K. Wang, B. Bauer, R.J.L. Townshend, S.A. Hollingsworth, J. E. Olivieri, H.E. Xu, Martha E. Sommer, R.O. Dror, Molecular mechanism of GPCR-mediated arrestin activation, *Nature* 557 (2018) 452–456, <https://doi.org/10.1038/s41586-018-0077-3>.
- [32] X.T. Zhou, D.N. Chen, Z.Q. Xie, Z. Peng, K.D. Xia, H.D. Liu, W. Liu, B. Su, J.D. Li, Functional analysis of the distal region of the third intracellular loop of PROKR2, *JBC* 439 (2013) 12–17, <https://doi.org/10.1016/j.bbrc.2013.08.039>.